

NASA Technical Memorandum

NASA TM-86466

(NASA-TM-86466) A REVIEW OF MICROMETEOROID
FLUX MEASUREMENTS AND MODELS FOR LOW ORBITAL
ALTITUDES OF THE SPACE STATION (NASA) 27 p
HC A03/MF A01 CSSL 22B

N84-33455

Unclas

G3/18 24017

A REVIEW OF MICROMETEOROID FLUX MEASUREMENTS
AND MODELS FOR LOW ORBITAL ALTITUDES
OF THE SPACE STATION

By Michael Susko ✓
Systems Dynamics Laboratory

September 1984



NASA

National Aeronautics and
Space Administration

George C. Marshall Space Flight Center

1. REPORT NO. NASA TM-86466	2. GOVERNMENT ACCESSION NO.		3. RECIPIENT'S CATALOG NO.	
4. TITLE AND SUBTITLE A Review of Micrometeoroid Flux Measurements and Models for Low Orbital Altitudes of the Space Station			5. REPORT DATE September 1984	
			6. PERFORMING ORGANIZATION CODE	
7. AUTHOR(S) Michael Susko			8. PERFORMING ORGANIZATION REPORT #	
9. PERFORMING ORGANIZATION NAME AND ADDRESS George C. Marshall Space Flight Center Marshall Space Flight Center, Alabama 35812			10. WORK UNIT NO.	
			11. CONTRACT OR GRANT NO.	
			13. TYPE OF REPORT & PERIOD COVERED Technical Memorandum	
12. SPONSORING AGENCY NAME AND ADDRESS National Aeronautics and Space Administration Washington, D.C. 20546			14. SPONSORING AGENCY CODE	
15. SUPPLEMENTARY NOTES Prepared by Systems Dynamics Laboratory, Science and Engineering.				
16. ABSTRACT A review of meteoroid flux measurements and models for low orbital altitudes of the Space Station has been made in order to provide information that may be useful in design studies and laboratory hypervelocity impact tests which simulate micrometeoroids in space for design of the main wall of the Space Station. This report deals with the meteoroid flux mass model, the defocusing and shielding factors that affect the model, the probability of meteoroid penetration of the main wall of a Space Station. Whipple (1947) suggested a meteoroid bumper, a thin shield around the spacecraft at some distance from the wall, as an effective device for reducing penetration, which has been discussed in this report. The equations of the probability of meteoroid penetration, the average annual cumulative total flux, ϕ , and the equations for the thickness of the main wall and the bumper are presented in this report. NOTE: Space debris has become a subject of increasing concern during the past decade. It is not covered in this report but information on the flux of orbital debris must be included in any final Space Station structural design or protection consideration in addition to the micrometeoroid flux of the natural environment.				
17. KEY WORDS Micrometeoroids Space Station Structures			18. DISTRIBUTION STATEMENT Unclassified - Unlimited	
19. SECURITY CLASSIF. (of this report) Unclassified	20. SECURITY CLASSIF. (of this page) Unclassified		21. NO. OF PAGES 26	22. PRICE NTIS

ACKNOWLEDGMENTS

The author wishes to express his appreciation to Dr. William G. Johnson of NASA-Marshall Space Flight Center for reviewing and contributing to this report. Special thanks go to Dr. William W. Vaughan for his encouragement in writing this report. The constructive suggestions and comments of Mr. Burton Cour-Palais of NASA-Johnson Space Center were also helpful in the development of the report.

TABLE OF CONTENTS

	Page
I. INTRODUCTION	1
II. DISCUSSION - METEORIODS.....	1
III. TOTAL METEOROID FLUX MASS MODEL	6
IV. PROBABILITY OF METEOROID PENETRATION	11
V. METEOROID PENETRATION - BUMPER AND MAIN WALL	12
VI. UNCERTAINTY IN HYPERVELOCITY LABORATORY STUDIES.....	14
VII. CONCLUDING REMARKS	15
REFERENCES	17
APPENDIX A - NATURAL ENVIRONMENT DESIGN CRITERIA FOR THE SPACE STATION PROGRAM DEFINITION PHASE	21

LIST OF ILLUSTRATIONS

Figure	Title	Page
1.	Terrestrial mass-influx rates of meteoroids.....	3
2.	Cumulative particle fluxes from various data sources.....	4
3.	Elemental composition of micrometeoroid residue found in the crater.....	5
4.	Comparison of cumulative sporadic meteoroid flux-mass data and the adopted sporadic model	8
5.	Average cumulative total meteoroid flux-mass model for 1 A.U.....	9
6.	Defocusing factor due to Earth's gravity for average meteoroid velocity of 20 km/s.....	10
7.	Method for determining body shielding factor for randomly oriented spacecraft	11

TECHNICAL MEMORANDUM

A REVIEW OF MICROMETEOROID FLUX MEASUREMENTS AND MODELS FOR LOW ORBITAL ALTITUDES OF THE SPACE STATION

I. INTRODUCTION

The Space Station Program Elements (SSPE's) micrometeoroid environment design criteria is presented in NASA Technical Memorandum 86460, "Natural Environment Design Criteria for the Space Station Program Definition and Preliminary Design (First Revision)," Vaughan (1984). Appendix A is an excerpt from the section in this report on the subject. Although the orbital altitudes are not yet precisely defined due to the evolutionary configuration of the Space Station, the lower and upper limits of the orbital altitudes will be based on the constraints set by the drag and orbital decay of the Space Station and payload delivery of weight to orbit criteria by the Shuttle. With these constraints, the lower and upper limits of the orbital altitudes of the Space Station may be between 250 n.mi. \approx 460 km and 300 n.mi. \approx 555 km, Susko (1984).

This report is intended as a review and summary of information available on meteoroid flux. No new measurements have become available for analysis in recent years. In addition, the subject of space orbital debris has increased in importance during the past decade and further complicates the matter of orbital design and protection from damage. A description of meteoroids is presented in Section II. The total meteoroid flux mass model and the probability of meteoroid penetration of the bumper and main wall of the Space Station are discussed in Sections III, IV, and V. Section VI gives the uncertainty in hypervelocity impact studies and Section VII lists the concluding remarks.

II. DISCUSSION - METEOROIDS

Meteoroids are extraterrestrial matter larger than molecular scale in size. The solid objects encompassed by the term "meteoroids" range in size from microns to kilometers and in mass from $\leq 10^{-12}$ g to $\geq 10^{16}$ g. Those less than 1 gram are often called "micrometeoroids." If objects of more than approximately 10^{-6} g mass reach Earth's atmosphere, they are heated to incandescence, producing the visible effect called a "meteor." If the initial mass and composition permits some of the original meteoroid to reach Earth's surface unvaporized, the object is called a "meteorite."

Meteorites are thought to derive primarily from comets and asteroids with perihelia near or inside Earth's orbit. The original objects were supposedly broken down into a distribution of smaller bodies by collisions. Meteoroids recently formed still tend to be concentrated near the orbital path of their parent body. These "stream meteoroids" produce the well known meteor showers which occur at certain dates and from particular directions. Table 1, from NASA TM-82478, Burbank, et al., (1965), and Millman (1978) lists the major meteoroid streams.

The average hourly rate of meteoroids increases at times during a calendar year due to meteoroid streams as previously noted. Their periods of activity and peak fluxes are given in Table 1, where F_{\max} is the ratio of the stream to the sporadic

TABLE 1. MAJOR METEOROID STREAMS

Name	Period of Activity	Date of Activity	F_{\max} Maximum	Geocentric Velocity (km/sec)
Quadrantids	January 2 to 4	January 3	8.0	42
Lyrids	April 19 to 22	April 21	0.85	48
η -Aquarids	May 1 to 8	May 4 to 6	2.2	64
O-Cetids	May 14 to 23	May 14 to 23	2.0	37
Arietids	May 29 to June 19	June 6	4.5	38
ζ -Perseids	June 1 to 16	June 6	3.0	29
β -Taurids	June 24 to July 5	June 28	2.0	31
δ -Aquarids	July 26 to August 5	July 8	1.5	40
Perseids	July 15 to August 18	August 10 to 14	5.0	60
Orionids	October 15 to 25	October 20 to 23	1.2	66
Arietids, southern	October through November	November 5	1.1	28
Taurids, northern	October 26 to November 22	November 10	0.4	29
Taurids, night	November		1.0	37
Taurids, southern	October 26 to November 22	November 5	0.9	28
Leonids, southern	November 15 to 20	November 16 to 17	0.9	72
Bielids	November 12 to 16	November 14	0.4	16
Geminids	November 25 to December 17	December 12 to 13	4.0	35
Ursids	December 20 to 24	December 22	2.5	37

F_{\max} is the ratio of average maximum cumulative stream to average sporadic flux for a mass of 1 g and a velocity of 20 km/sec.

meteoroid cumulative flux levels. Note that there is little or no enhancement of the sporadic population for masses less than 10^{-6} gm during stream activity.

Meteoroids are assumed to be spherical in shape and to have a bulk mass density of 0.5 gm/cc. However, this does not apply to micrometeoroids ($<50 \mu$ diameter) and it is generally assumed that a density of 2 gm/cc is more appropriate. The average atmospheric entry velocity of sporadic meteoroids is 20 km/s, which is the value generally used to assess impact damage to spacecraft in Earth orbit. Stream meteoroids generally enter much faster as seen in Table 1.

Meteoroids may be classified by composition: stony, iron, and perhaps, icy. From their composition, the type of parent body can be inferred. Meteoroids are attracted by the Earth's gravity field so that the flux from allowed directions in near-Earth orbit is increased by approximately 1.7 over the interplanetary value. The Earth also shields certain arrival directions.

The total mass infall to Earth is estimated to be 10^{10} g/year. Figure 1 shows the distribution of number with mass, where $N(\geq m)$ is the number flux with mass $\geq m$, Gault (1970). The flux is low and, therefore, difficult to measure. Evidence includes: spherules on the sea floor and the polar icecaps, impacts detected with special sensors on satellites, meteor trails in the atmosphere observed visually by radar, lunar crater accounts, and zodiacal lights, Bless, et al. (1972) and Kessler, et al. (1980, 1968). The fluxes of Figure 1 are probably uncertain by a factor of 10.

A review of meteoroid flux measurements by various experimenters, who contributed to the meteoroid flux measurements as presented in Figure 1, are as follows: The implied meteoroid flux measurements by Brownlee, et al. (1971) were in general agreement with Spacecraft Pioneer 8, 9, Cosmos 163, and Pegasus. Brownlee, et al. (1967), as guest experimenters on the Gemini S-12 micrometeorite-collection program, obtained space density of particles consistent with satellite-penetration data. Hodre,

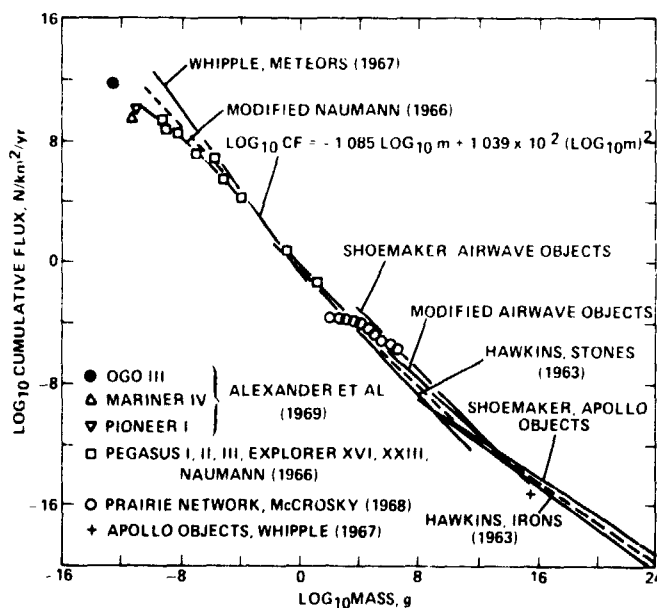


Figure 1. Terrestrial mass-influx rates of meteoroids. N is the flux of particles with mass greater than m [Gault (1970)].

et al., (1972) performed optical and scanning electron microscope examination of four glass filters brought back by the Apollo 12 mission. No primary hypervelocity crater were found and this fact provided an upper limit to the flux of micrometeoroid particles impacting the lunar surface that is low and that agrees well with results from Pegasus, Pioneer 8/9, and Cosmos spacecraft as shown in Figure 1. Flux measurements by Whipple (1967), Naumann (1966), Shoemaker (1965), Hawkins (1963), Alexander, et al (1969), were valuable contributors to the micrometeoroid flux measurements. Davidson (1963) reported on the effect of meteoroid flux variations on the reliability of space vehicles.

Figure 2 shows a compilation of data for near-Earth space derived by various means over a more restricted mass range than Figure 1. (The fluxes shown in Figs. 1 and 2 are 1 year averages.) The flux for $m < 10^{-12}$ g is rather uncertain. There have been estimates of micrometeoroid flux a factor of 10 higher than those in Figure 1 [McDonnell (1976)]. This appears to be a real uncertainty.

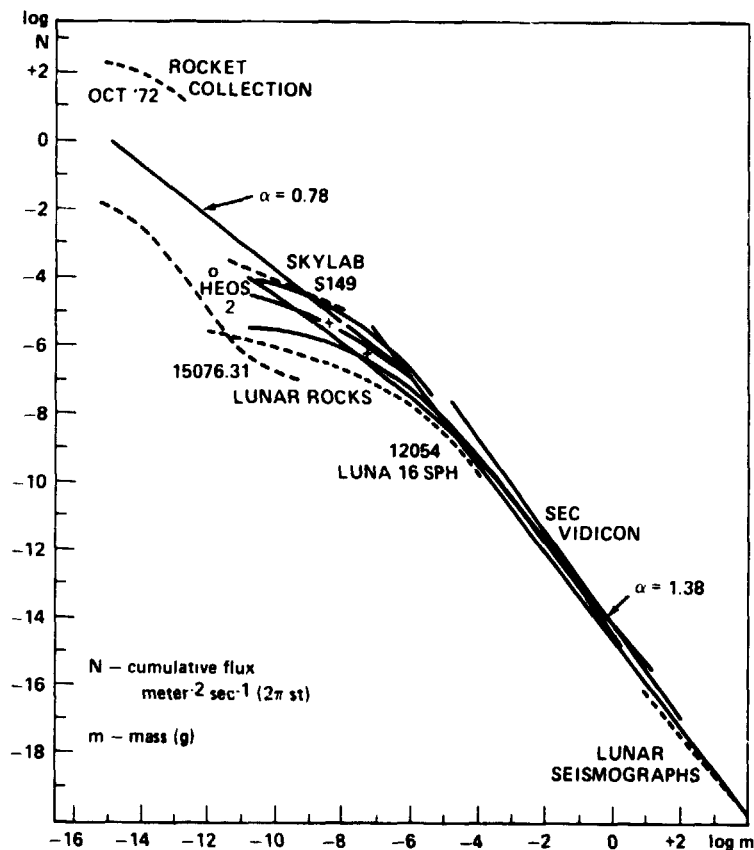


Figure 2. Cumulative particle fluxes from various data sources [Fields and Cameron (1976)].

Brownlee, et al. (1974) and Lundquist (1979) presented measurements of elemental abundances in typical high velocity impact craters from micrometeoroids in Skylab's near-Earth orbit. Considerable amounts of micrometeoroid residue were found in the bottom of rough-textured craters.

ORIGINAL PAGE IS
OF POOR QUALITY

The results of two electron-probe analyses are shown in Figure 3, the relative abundance being normalized to the amount of silicon found. Elements identified were iron, silicon, magnesium, calcium, nickel, chromium, and manganese. Upper limits were also obtained for titanium and cobalt. For comparison, the relative elemental abundances for two types of carbonaceous chondrite meteorites (C1 and C3) are also given. There is a marked similarity, but this should not be construed as evidence that both objects have a common source. The similarities are possibly only a consequence of their both being primitive, well-preserved samples of early solar system materials. A sulfur analysis at a later date indicated that sulfur is also present in the crater with an abundance similar to the abundances of iron, magnesium, and silicon and also comparable to the abundances for carbonaceous chondrites.

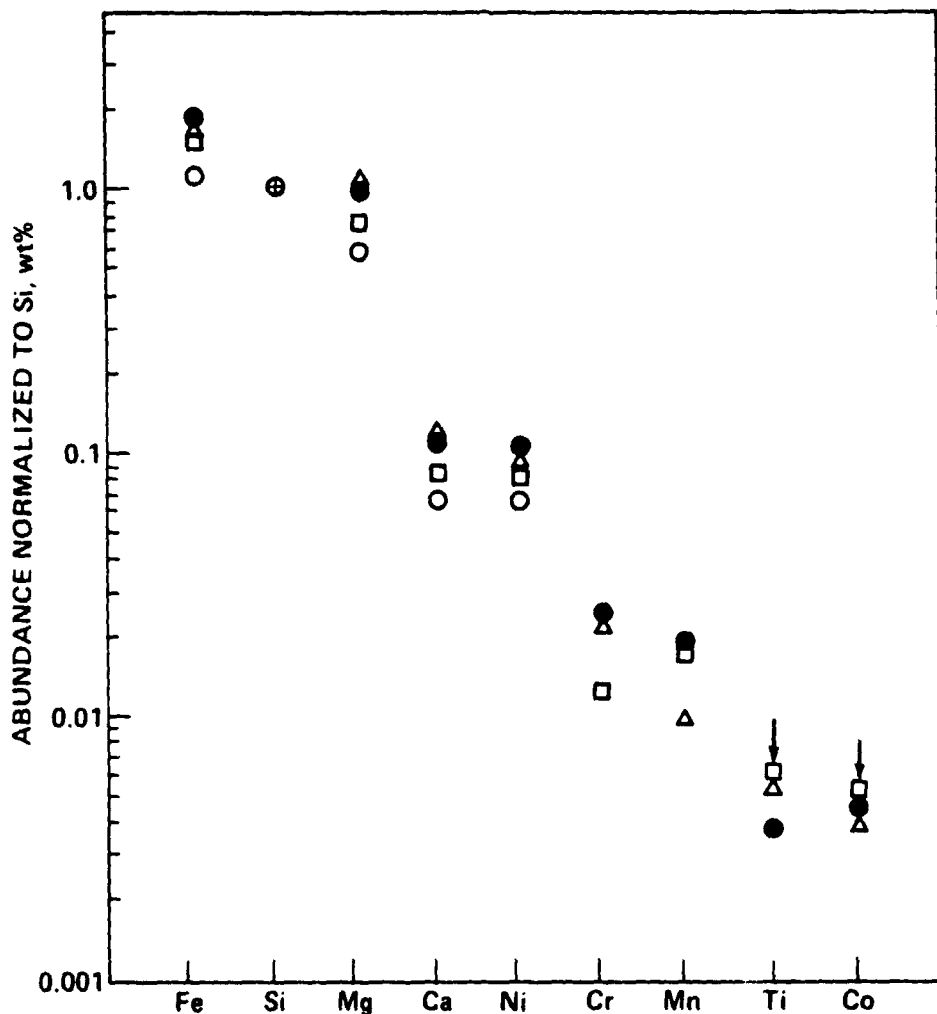


Figure 3. Elemental composition (normalized to silicon) of micrometeoroid residue found in the crater. The open squares and circles represent different electron-beam probe runs. The elemental compositions of two types of carbonaceous chondrite meteorites (C1 and C3), represented by solid circles and by crosses, respectively, are shown for comparison.

(+)

Further information on meteoroid impact will be obtained from the Long Duration Exposure Facility (LDEF) NASA SP-473 (1984) which will be flown for one year (lift-off in April, 1984). The LDEF opportunity is a retrievable spacecraft. It will allow investigators to gather data over a long period of time (approximately one year) and have their experiments returned for an in-depth analysis, increasing the different kinds of testing and the number of investigators. The micrometeoroid experiment on LDEF will use an aluminum plate as a detector to estimate the population and size distribution of meteoroids and space debris near Earth. The craters will be analyzed by X-ray spectroscopy, determining the abundance and the different elements. The impacting particle material will be used to distinguish between meteoroid craters and those caused by man-made debris.

Because of flexibility in analysis, recoverable crater collection experiments are subject to fewer uncertainties in detection of impacts than are remote sensing experiments. Studies like the Skylab experiments provide a permanent record of impact events which can be analyzed under laboratory conditions to yield information on particle mass, density, shape composition and velocity. Crater collection experiments also record impacts of particles too small or of too low density to register on existing remote sensing experiments. This information will be used to update the NASA Technical Memorandum 82478, Space and Planetary Environment Criteria Guidelines for Use in Space Vehicle Development, 1982 Revision (Volume 1).

III. TOTAL METEOROID FLUX MASS MODEL

From NASA SP-8013 (1969) the logarithms of the flux and mass values from Table 2 are plotted in Figure 4. Uncertainty in the directly measured flux is small (< 10 percent) as a result of the large number of penetrations obtained on each sensor system. The characteristic mass for the threshold penetration is probably correct within a factor of three.

The data from the 0.046 cm sensor on Pegasus II and III have been used to establish another point for the model. A cumulative flux of 8.00×10^8 particles per square meter per second from a mass of 10^{-6} gram or greater was adopted (point B in Fig. 4).

The data from Explorer XVI and XXIII are considered to be the most reliable and, as shown in Figure 4, are consistent in showing a decrease in the slope of the flux-mass relationship in the mass range 10^{-9} to 10^{-8} gram. Assuming the adopted flux at 10^{-6} gram is reliable, the decrease in slope is in agreement with the evidence provided by the intensity of zodiacal light and the concept of its physical limit to the amount of particulate debris in the solar system. Further indication of the slope trend is provided by the Ariel II results of Jennison (1967). Accordingly, the Explorer data points have been used to determine the shape of the flux-mass curve at masses less than 10^{-6} g.

The summary of the model development as pointed out in NASA SP-8013 (1969) in the mass range 10^{-6} and greater (points A to B in Fig. 4), a straight line variation has been assumed; in the range 10^{-6} gram and less, where the penetration data indicated a decrease in the slope of the flux-mass relationship with decreasing mass,

TABLE 2. SPORADIC FLUX-MASS DATA FROM PENETRATION MEASUREMENTS

SPACECRAFT	SENSOR MATERIAL	K ₁	SENSOR THICKNESS t (cm)	CHARACTERISTIC MASS m (gm)	CUMULATIVE FLUX ϕ ($m^{-2} \text{-sec}^{-1}$)	LOG ₁₀ m (gm)	LOG ₁₀ ϕ ($m^{-2} \text{-sec}^{-1}$)
PEGASUS I,II,III	ALUMINUM 2024-T3	0.54	0.0406	5.20 X 10 ⁻⁷	8.00 X 10 ⁻⁸	-6.28	-7.10
			0.0203	7.25 X 10 ⁻⁸	3.44 X 10 ⁻⁷	-7.14	-6.46
EXPLORER XXIII	STAINLESS STEEL TYPE 302	0.32	0.0051	6.29 X 10 ⁻⁹	3.33 X 10 ⁻⁶	-8.20	-5.48
			0.0025	8.28 X 10 ⁻¹⁰	5.68 X 10 ⁻⁶	-9.08	-5.25
EXPLORER XVI	BERYLLIUM COPPER BERYLCO NO. 25	0.30	0.0051	7.55 X 10 ⁻⁹	2.66 X 10 ⁻⁶	-8.12	-5.58
			0.0025	9.95 X 10 ⁻¹⁰	5.16 X 10 ⁻⁶	-9.00	-5.29

ORIGINAL PLOT
OF POOR QUALITY

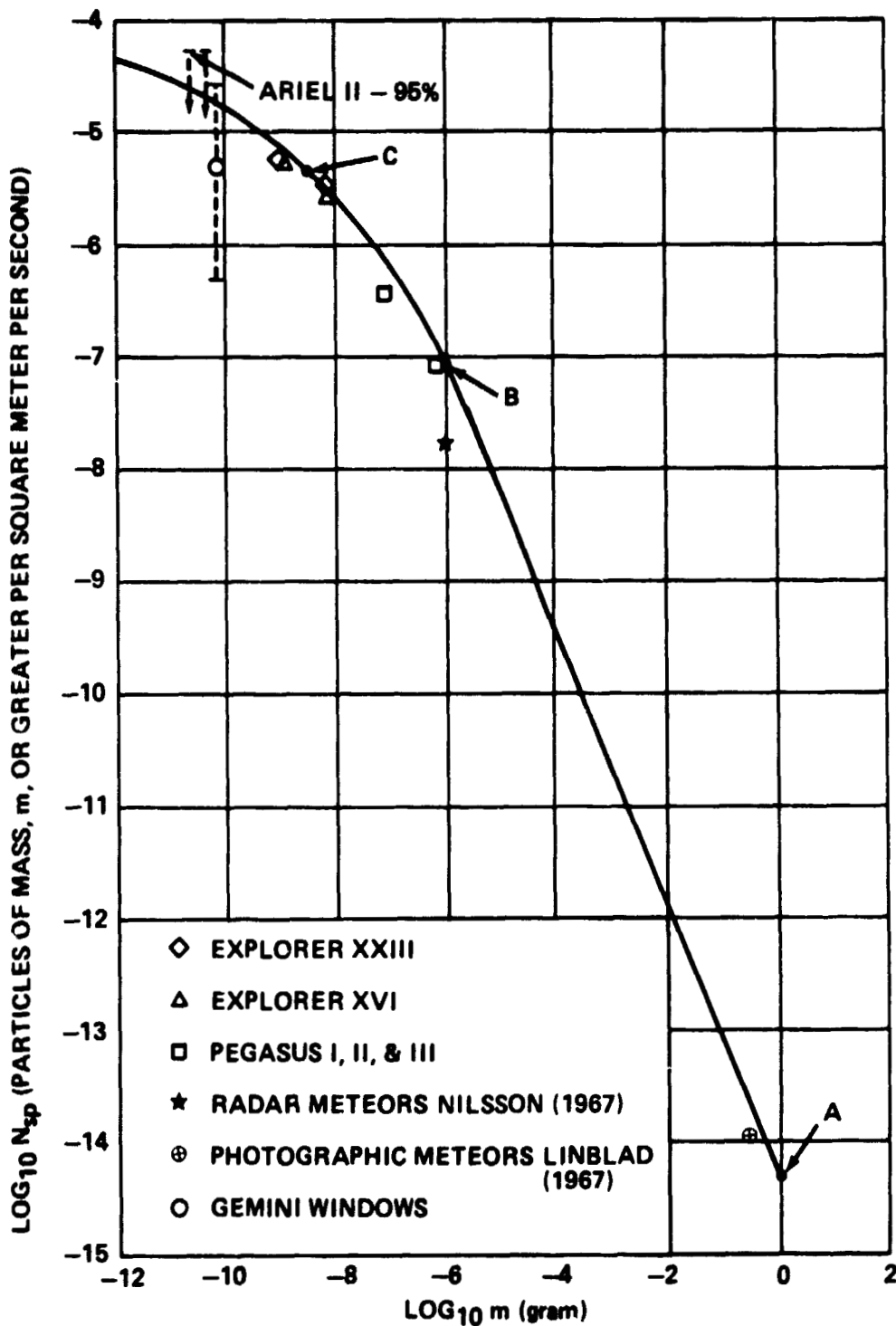


Figure 4. Comparison of cumulative sporadic meteoroid flux-mass data and the adopted sporadic model.

ORIGINAL PAGE IS
OF POOR QUALITY

a non-linear variation passing through the Explorer data has been adopted between 10^{-6} to 10^{-12} gram. At the latter mass, the model was arbitrarily terminated. At point C in Figure 4, a cumulative flux of 3.98×10^{-6} particles per square meter per second together with a mass of 2.5×10^{-9} grams was chosen to best fit all four of the Explorer data points in determining an equation for the non-linear variation. The model along with the applicable mathematical equations is shown in Figure 5, NASA SP-8013 (1969); Naumann et al., (1971); Clifton (1973); and Brooks (1976).

The well-known meteor showers shown in Table 1, which occur at certain dates and from particular directions are included in Figure 5, resulting in a 10 percent increase in average flux due to the major meteoroid streams, NASA SP-8013 (1969).

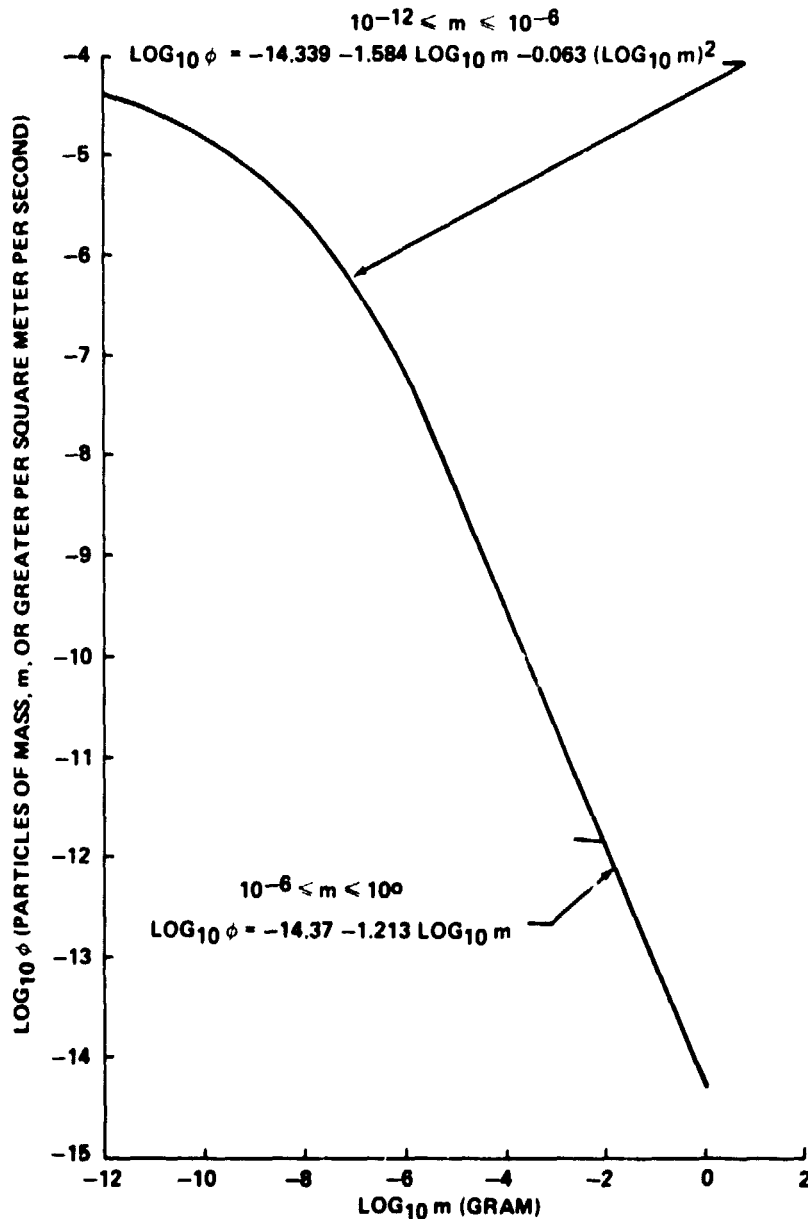


Figure 5. Average cumulative total meteoroid flux-mass model for 1 A.U.

ORIGINAL PAGE IS
OF POOR QUALITY

The number-mass distribution of meteoroids up to 1 g at 1 A.U. (the Earth's orbit) has been modeled in Reference NASA SP-8013 (1969) and the results are shown in Figure 5 [Brooks (1976)] where number densities (particles/m³) have been multiplied by a constant speed of 20 km/s to compute incident flux, ϕ . This flux is assumed to be isotropic, on the average, with respect to randomly oriented objects. For spacecraft in orbit around the Earth, the flux values in Figure 5 for any given cumulative mass (i.e., the flux for all meteoroids greater than or equal to a given mass) must be multiplied by a defocusing factor G, Figure 6, a shielding factor, δ , Figure 7, to account for the Earth's gravitational focusing of meteoroids and also for the shielding provided by the Earth as presented in NASA SP-8013 (1969).

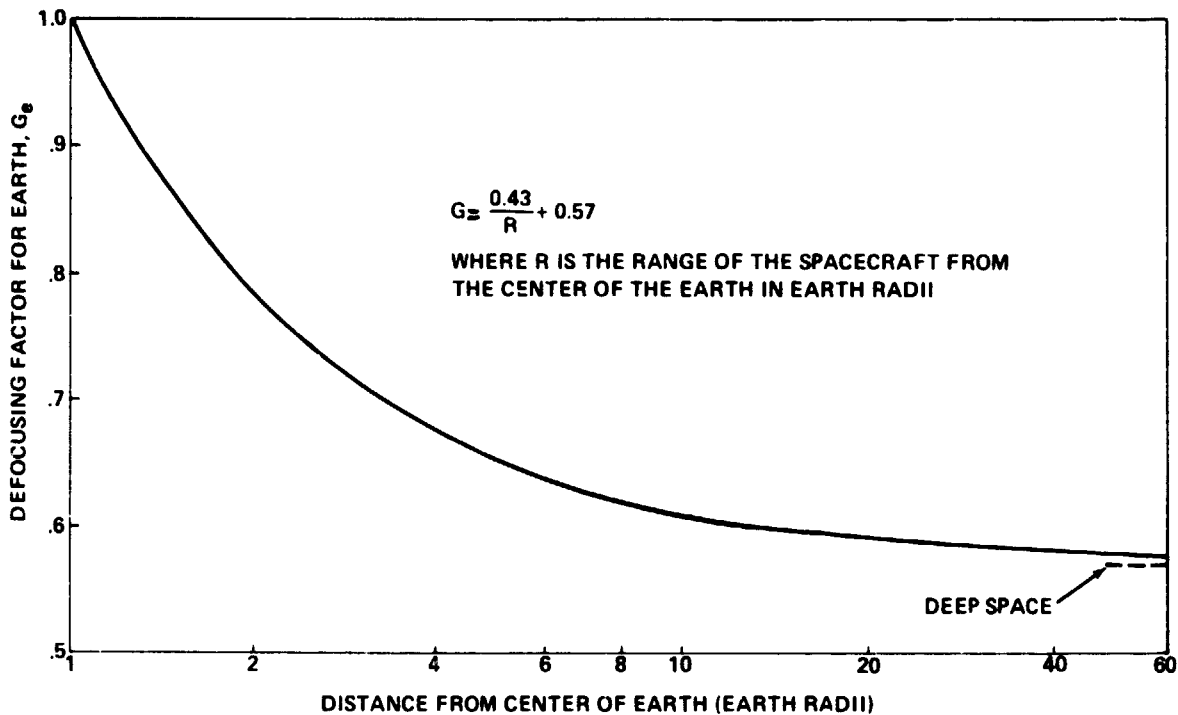


Figure 6. Defocusing factor due to Earth's gravity for average meteoroid velocity of 20 km/s.

The model states that the average annual cumulative total flux, ϕ , in impacts/m²s of meteoroids of mass m and greater in gram on a spacecraft is

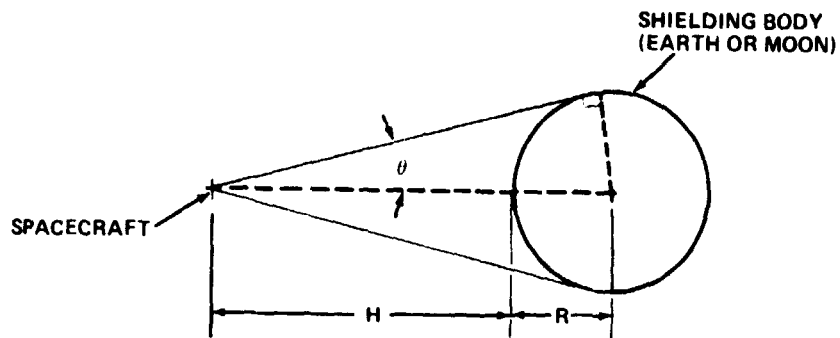
$$\phi = G \zeta 10^{[-14.339 - 1.584 \log_{10} m - 0.063 (\log_{10} m)^2]} \quad (1)$$

for m between $10^{-12} \leq m \leq 10^{-6}$, and

$$\phi = G \zeta 10^{(-14.37 - 1.213 \log_{10} m)}$$

for m between $10^{-6} \leq m \leq 10^0$.

ORIGINAL
OF POOR QUALITY



BODY SHIELDING FACTOR, ζ : (DEFINED AS RATIO OF THE SHIELDED TO UNSHIELDED FLUX)

$$\zeta = \frac{1 + \cos \theta}{2}$$

WHERE:

$$\sin \theta = \frac{R}{R + H} \quad , \quad \theta = \sin^{-1} \left(\frac{R}{R + H} \right)$$

R RADIUS OF SHIELDING BODY
H ALTITUDE ABOVE SURFACE

SUBSCRIPTS:

e EARTH
m MOON

Figure 7. Method for determining body shielding factor for randomly oriented spacecraft.

IV. PROBABILITY OF METEOROID PENETRATION

The probability of meteoroid penetration (assuming that this number is less than 1) is related to flux through a Poisson distribution presented by Cour-Palais (1969) in [NASA SP-8013 (1969); Humes (1981)].

$$P_p = \phi_p A t e^{-\phi_p A t} = \phi_p A t (1 - \phi_p A t + \phi_p^2 A^2 t^2 - \dots) \quad (2)$$

where

P = probability of penetration

ϕ = flux against a spacecraft structure, impacts per m^2 per s

A = area of a spacecraft structure, m^2

t = time, s

Subscript p = penetration .

One of the factors in establishing the area of the space station is that the view of space from the modules may be partially obstructed by other modules so that the effective area of each module is less than its actual area. For micrometeoroids approaching with equal probability from all directions, the effective area of a cell from Humes (1981) is,

$$A_{\text{eff}} = \int_{x=0}^w \int_{y=0}^l \int_{\gamma=0}^{\pi/2} f_1(\gamma, y, x) \cos \gamma \, d\gamma \, dy \, dx$$

$$+ \int_{x=0}^w \int_{y=0}^l \int_{\gamma=0}^{\pi/2} f_2(\gamma, y, x) \cos \gamma \, d\gamma \, dy \, dx \quad (4)$$

where

γ = the view angle of space measured from the normal to the surface

$f_1(\gamma, x, y)$ = the fraction of the view angle γ (from a point x, y) in the module that is obstructed by other spacecraft components on one side of the module

$f_2(\gamma, x, y)$ = the corresponding function for the other side of the panel

w = the width of the module

l = length of the module.

The $\cos \gamma$ appears in equation (2) because the projected area of the surface element depends on the viewing angle.

V. METEOROID PENETRATION - BUMPER AND MAIN WALL

An empirical equation based on hypervelocity impacts used to establish a characteristic mass for threshold penetration of the detector panels employed on the Pegasus and Explorer meteoroid detection satellites was determined by Naumann, et al., (1969) and presented in NASA SP-8013 (1969) is as follows:

$$t = K_1 \rho^{1/6} m^{0.352} v^{0.875}$$

where

t = the thickness of the plate penetrated (cm)

K_1 = a constant

ρ = the mass density of the meteoroid (g/cm^3)

m = the mass of the meteoroid (g)

v = the normal impact velocity of the meteoroid (km/s).

The constant, K_1 , is a characteristic of the plate material. It reflects the combined effects of the material strength, density, ductility, and temperature on threshold penetration as determined from hypervelocity tests. In applying the equation, ρ was taken as 0.5 g/cm^3 (the chosen average mass density of meteoroids), v as 20 km/s (the adopted average velocity of sporadic meteoroids), and K_1 as determined from hypervelocity impact tests on materials. Table 2 presents the calculated characteristic mass for the sensors indicated, the value of K_1 for each sensor material involved, and the cumulative flux as determined from each penetration sensor system.

As indicated in NASA SP-8013 (1969), conversion of penetration data from sensor material thickness to particle mass has been accomplished by calculating the critical mass that will just perforate the sensor thickness in question. Currently, no direct experimental determination of the critical mass is possible at the average impact velocity of sporadic meteoroids which is 20 km/s . Velocities of 7.5 to 12 km/s and extrapolation of these laboratory velocities to average meteoroid velocities are used to obtain critical mass, Naumann (1966) and Fish and Summers (1965).

Whipple (1947) suggested that damage to a spacecraft from a meteoroid impact could be greatly reduced by placing a thin shield around the spacecraft at some distance from the hull. Whipple envisioned that this shield, which he called a meteor bumper, would vaporize meteoroids upon impact thus dissipating their penetrating powers. Theoretically, the function of the bumpers is to generate a shock wave which compresses the material and then a release wave fragments the material into small pieces.

The principle of the micrometeoroid shield was shown experimentally during the Skylab IV tests of stacked gold foils over stainless steel substrate. A micrometeoroid struck the first gold foil and shattered into fragments, which in turn penetrated the second gold foil. The micrometeoroid must have been quite fragile, since it fragmented upon striking a foil much thinner than its dimension. In one case, two small craters were found in the stainless steel substrate after a particle penetrated two layers of gold foil. Fragmentation of micrometeorites striking the shield would greatly reduce the possibility of damage to the spacecraft wall. Although Skylab's 0.6 mm -thick micrometeoroid shield was lost, the orbital workshop's 3.18 mm thick wall was not penetrated during the 67 day Skylab IV mission, indicating there was little meteoroid hazard with such wall thickness.

Essentially Humes (1981) indicated that the bumper concept was demonstrated in a number of laboratory tests. Even at an impact speed too low to cause vaporization, a bumper was seen to fragment the projectile and disperse the fragments over a large area of the main wall, giving the double-wall structure a much greater resistance to penetration than a single wall of the same thickness. As indicated by Humes (1981), all the laboratory tests were conducted at impact speeds less than the average meteoroid impact speed, and it is unclear how the data should be extrapolated to meteoroid velocities.

Experimental hypervelocity impact studies of the bumper and main wall impact were made by Swift (1983); Humes (1981, 1969, 1965, 1963); Nysmith (1969); Naumann, et al., (1969); Madden (1967); Jex, et al. (1970); Cour-Palais (1979, 1973, 1969); and others.

Swift, et al., (1983) presented a new analysis for designing dual layer shields based on energy and momentum conservation, fundamental electromagnetic radiation physics and the observation of results of extensive experimental impact studies performed at relatively low velocities near 7 km/s. Equation (5) follows:

$$r_c = r_m \left(\frac{\rho_m U_m^2}{R} \right)^{1/3} \quad (5)$$

Equation (5) is the direct consequence of the fact that impact crater volume is nearly proportional to the kinetic energy of the impactor, with the proportionality factor being dependent upon materials properties of both the impactor and target. The proportionality constants are approximately $R = 10^{10}$ erg/cm³ (10^9 J/m³) for low density projectiles striking hard aluminum targets. Now,

r_m = meteoroid radius

ρ_m = density of meteoroid material

U_m = meteoroid velocity

r_c = impact crater radius (depth) .

The impact threat and the resulting impact crater radius (depth) to the main wall from the meteors passing holes in the bumper plate can be predicted using equation (5) [Swift, et al. (1983)].

The above relationship may be extended slightly to evaluate the ballistic limit thickness of the underlying plate (main wall) by noting that plates 1.5 times as thick as the crater depth are usually needed to achieve ballistic limit conditions as presented in equation (6).

Equation (6) may be used to determine the ballistic limit size for meteoroids impacting with the bumper plate. Again, a value of $R = 10^{10}$ ergs/cm³ is appropriate for most such calculations where near optimum shield configurations are being considered. Equation (6) follows:

$$d_{bl} = \frac{3r_m}{2} \left(\frac{\rho_m U_m^2}{R} \right)^{1/3} \quad (6)$$

where

d_{bl} = ballistic limit thickness.

Extrapolation of equation (6) to the velocity ranges typical of meteoroid impacts in near-Earth space produces results which are intuitively reasonable, according to Swift, et al. (1983).

VI. UNCERTAINTY IN HYPERVELOCITY LABORATORY STUDIES

The greatest uncertainty in hypervelocity laboratory experiments is the mass of the projectile, not knowing how much material is ablated by the drag acceleration. According to Naumann, et al. (1969), one of the major difficulties in calibrating the flight detectors lies in the very small particle sizes that must be used. Particles as small as 20 microns were used for the thinnest detector samples. With such sizes there is no method of photographing the projectile just prior to impact, as is standard procedure in most hypervelocity ranges. Even if such a particle could be resolved, at 10 km/s it travels its own diameter in 2 nanoseconds, which makes it beyond the state of the art to stop its motion. In any launch process there is fine, high-velocity debris from gun parts, fragmented projectiles, sabot fragments, etc. In dealing with larger projectiles, the presence of such debris is not usually a problem since the damage from the projectile can be distinguished from the debris. However, when the projectile size is smaller than some of the debris, it becomes very difficult to make such a determination.

VII. CONCLUDING REMARKS

The meteoroid flux mass model, the defocusing and shielding factors that affect the model, and the probability of penetration equations for design of the main wall of the space station have been presented. The review of meteoroid flux measurements and models for low orbital altitudes has revealed three things that may damage the main wall of the Space Station if a meteoroid passes through the bumper. They are:

- 1) The meteoroid fragments individually might penetrate the main wall.
- 2) Meteoroid fragments collectively can strike the main wall like a pressure pulse, and may make the main wall bulge, crack, and petal open.
- 3) Bumper fragments might individually penetrate the main wall depending upon its design capability.

Experiments by Whipple (1947, 1967); Humes (1981, 1969, 1965, 1963); Madden (1967); Naumann (1969); Nysmith (1969); Swift (1983); and Jex (1970) were conducted at impact speeds less than the average meteoroid impact speeds, and it is unclear how the data should be extrapolated to meteoroid velocities. Essentially, the experiments were designed to compute a critical thickness of the bumper, and a critical distance between the bumper and main wall and the thickness of the main wall. Kessler (1980, 1978, 1972) presented information on the debris resulting from rocket explosions and the trend for collisions between orbiting fragments. Cour-Palais, et al (1972) and Flaherty, et al. (1970) gave results of impact damage to Surveyor 3 and Gemini spacecraft, respectively. Pioneer work in meteoroid flux measurements was done by Davidson (1963, 1968).

A NASA workshop on "Space Debris and Meteoroid Technology and Implications to Space Station" was held September 5-6, 1984, at NASA's Marshall Space Flight Center. It was sponsored by the NASA Office of Aeronautics and Space Technology and included participation from the Jet Propulsion Laboratory, Ames Research Center, Johnson Space Center, Langley Research Center, Marshall Space Flight Center, and Army's Corps of Engineers.

The participants discussed the general technology status of both the environment definition and the capabilities to protect the Space Station Program Elements against the full range of predicted particle masses and velocities. The general technology needs as reflected in the minutes of the workshop in order of priority are:

1) Improve the definition and confidence of predicting the space debris environment during the orbital lifetime of the Space Station.

2) Develop criteria for design and testing of Space Station subsystem hardware. Establish trade-offs for determining desired protection levels versus criticality in conjunction with replaceability and redundancy options.

3) Define by test secondary effects of meteoroid or space debris impact, especially penetration into a cabin atmosphere, using hypervelocity test facilities. Upgrade and maintain the existing NASA light gas gun facilities and instrumentation to support all necessary testing.

4) Assess applicability of advanced armor concepts to Space Station wall designs. Investigate long duration meteoroid exposure effects on windows, vulnerable surfaces such as radiators, thermal coatings, and solar arrays.

5) Determine the applicability of advanced hydrodynamic computer codes to supplement or replace hypervelocity impact testing.

REFERENCES

Alexander, W. M., Corbin, J. D., Arthur, C. W., and Bohm, J. L., 1969: Mariner IV and OGO III, Recent measurements of picogram dust particles flux in interplanetary and cislunar space. Twelfth Cospar meeting.

Anonymous, 1984: The long duration exposure facility (LDEF), Mission 1 Experiments. NASA SP-473.

Bless, R. C. and Savage, B. D., 1972: Interstellar extinction in the ultraviolet. The scientific results from the orbiting astronomical observatory (OAO-2), NASA SP-310.

Brooks, David R., 1976: A comparison of spacecraft penetration hazards due to meteoroids and manmade Earth-orbiting objects. NASA TM X-73978.

Brownlee, D. E., Tomandl, D. A., and Hodge, P. W., 1974: Elemental abundances in interplanetary dust. Nature, Vol. 252.

Brownlee, D. E., Bucker, W., and Hodge, P. W. (1971): Micrometeoroid flux from Surveyor glass surfaces. Proceedings of the Second Science Conference, Vol. 3, 2781-2789.

Brownlee, D. E., and Hodge, P. W. (1967): Gemini-12 meteoric-dust experiment results. Space Research VIII - North Holland Publishing Co., Amsterdam.

Burbank, P. B., Cour-Palais, B. G., and McAllum, W. E., 1965: A meteoroid environment for near-Earth cislunar and near-lunar operations. NASA TN D-2747.

Clifton, K. S., 1973: Television studies of faint meteors. Journal of Geophysical Research, Vol. 78, No. 28.

Cour-Palais, B. G., 1979: Space vehicle meteoroid shielding design. NASA, Lyndon B. Johnson Space Center, Houston, Tex., 80 N 22212.

Cour-Palais, B. G., 1973: Apollo window meteoroid experiment. NASA, Lyndon B. Johnson Space Center, Houston, Tex., 74 N 18453.

Cour-Palais, B. G., Flaherty, R. E., High, R. W., Kessler, D. J., McKay, D. S., and Zook, H. A. (1972): Results of examination of the returned Surveyor 3 samples for particulate impacts. NASA, Lyndon B. Johnson Space Center, Houston, Texas, N72-26731, 17-30.

Cour-Palais, B. G., 1969: Meteoroid environment model - 1969 (Near Earth to Lunar Surfaces), NASA SP-8013.

Davidson, J. R., 1968: The effects of the meteoroid environment parameters on single and double wall design. NASA, Langley Research Center, Hampton, VA, X71-71551.

Davidson, J. R., 1963: Environmental problems of Space Flight structures - part II, Meteoroid hazards. NASA TN-D-1493.

Davidson, J. R., 1963: The effect of meteoroid flux variations on the reliability of space vehicles. NASA Langley Research Center, Hampton, VA, X73-78708, 19-99.

Field, G. B. and Cameron, A. G. W. (eds.), 1975: The dusty universe, Neal Watson, Academic Publ., Inc., New York.

Fish, R. M. and Summers, J. L., 1965: The effect of material properties on threshold penetration. Proceedings of Seventh Hypervelocity Symposium, Vol. VI.

Flaherty, R. E., Kessler, D. J. and Zook, H. A. (1970): Meteoroid impacts on Gemini spacecraft windows, calculations flux-mass relation. Planetary and Space Science, Vol. 18, 953-964.

Gault, D. E., 1970: Saturation and equilibrium conditions for impact cratering on the lunar surface, Vol. 9, 215-238.

Hawkins, G. S., 1963: Impacts on the Earth and moon. Nature, 197, 781.

Hodge, P. W., Brownlee, D. E., and Bucher, W. (1972): Craters in Surveyor 3 glass surfaces. Space Research XII, Berlin, 1972.

Humes, D. H.: Meteoroid bumper experiment on Explorer 46, 1981, NASA Technical Paper 1879.

Humes, D. H., 1969: Calculation of the penetration flux for a multiwall structure on the lunar orbiter spacecraft, NASA TN D-5455.

Humes, D. H., 1965: The influence of the bumper and main wall material on the effectiveness of single meteoroids bumpers. NASA TN D-3104.

Humes, D. H., 1963: An experimental investigation of the effectiveness of single aluminum meteoroid bumpers, NASA TN D-1784.

Hemenway, C. L., 1971: The study of micrometeorite particle and new collection techniques, Cospar Space Research, 272-280.

Hemenway, C. L., Hallgren, D. S., Coon, R. E., and Bourdillon, L. A., 1967: Technical description of the Gemini S-10 and S-12 micrometeorites experiments. Space Research VII - North Holland Publishing Company, Amsterdam.

Jennison, R. C., McDonnell, J. A. M., and Rodgers, I., 1967: The Ariel II Micro-meteorite penetration measurements, Proceeding of the Royal Society, Vol. 300, 251-269.

Jex, D. W., Miller, A. M., and MacKay, C. A., 1970: The characteristics of penetration for a double-sheet structure with honeycomb. NASA TM X-53974.

Kessler, D. J., Landry, P. M., Gabbard, J. R., and Moran, J. L. T., 1980: Ground radar detection of meteoroids in space. Proceedings of the Symposium, Ottawa, Canada, August 27-30, 1979.

Kessler, D. J., 1980: Sources of orbital debris and projected environment for future spacecraft. AIAA, International meeting, Baltimore, MD.

Kessler, D. J., and Cour-Palais, B. G., 1978: Collision frequency of artificial satellites - The creation of debris belt. Journal of Geophysical Research, Vol. 83, 2637-2646.

- Kessler, D. J., 1972: A guide to using meteoroid environment models for experiment and spacecraft design applications. NASA TN-D6596.
- Kessler, D. J., 1968: Interplanetary dust - the zodiacal light and meteoroid measurements. OART-OSSA Meteoroid Environment Workshop, X71-71551.
- Lindblad, B. A., 1967: The luminosity function of sporadic meteors and the extrapolation of meteor influx rate to the micrometeorite region, NASA SP 135.
- Lundquist, C. A. (ed.), 1979: Skylab's astronomy and space sciences, NASA SP-404.
- Madden, R., 1967: Ballistic limit of double-walled meteoroid bumper system, NASA TN D-3916.
- McDonnell, J. A. (ed.), 1976: Cosmic dust, John Wiley and Sons, New York, Chapter 3, "Meteors" by D. W. Hughes; Chapter 6, "Microparticles studies by space instrumentation."
- Millman, G. H., 1979: HF scatter from overdense meteor trails. General Electric Co., Syracuse, N.Y., 79 N 10305.
- Nagel, K., Fechtig, H., Schneider, E., and Nauken, G., 1975: Micrometeorite impact craters on Skylab S-149, Max-Planck Institut für Kernphysik, Heidelberg, Germany.
- Naumann, R. J. and Clifton, K. S., 1971: Mass influx obtained from low light-level television observations of faint meteors. Evolutionary and Physical Properties of Meteoroids, IAU Colloquium 13, State University of N.Y. at Albany. NASA SP-319.
- Naumann, R. J., Jex, D. W., and Johnson, C. L. (1969): Calibration of Pegasus and Explorer XXIII detector panels, NASA TR R-321.
- Naumann, R. J., 1966: The near-Earth meteoroid environment, NASA Tech Note D-3717, Washington, D. C.
- Nilsson, C. S. and Southworth, R. B., 1967: The flux of meteors and micrometeoroids in the neighborhood of the Earth. Smithsonian Astrophysical Observatory Special Report No. 263.
- Nysmith, C. R., 1969: An experimental impact investigation of aluminum double-sheet structures, AIAA Hypervelocity Impact Conference, Cincinnati, Ohio, paper No. 69-375.
- Shoemaker, E. M., 1965: Preliminary analysis of the lunar surface in Mare Cognitum, Jet Propulsion Lab., Tech Rep. 32-700, Pasadena, California, 5-134.
- Smith, Robert E. and West, George S., 1983: Space and planetary environment criteria guidelines for use in space vehicle development, 1982 revision (volume 1). NASA TM-82478.
- Susko, Michael, 1984: Investigation of thermospheric winds relative to space station orbital altitudes, NASA TM-82577.
- Swift, H. F., Bamford, R., and Chen, R., 1983: Designing space vehicle shields for meteoroid protection: a new analysis. Adv. Space Res., Vol. 2, No. 12, 210-234.

Vaughan, W. W., 1984: Natural environment design criteria for the space station program definition and preliminary design (first revision), NASA TM-86460.

West, G. S., Jr., Wright, J. J., and Euler, H. C., 1977: Space and planetary environment criteria guidelines for use in space vehicle development, 1977 revision, NASA TM 78119.

Whipple, E. L., 1967: On monitoring the meteoritic complex. Smithsonian Observ. Special Rep. 239, Cambridge, Massachusetts, 2-45.

Whipple, E. L., 1947: Meteorites and space travel. Astron. J., Vol. 52, 5-131.

APPENDIX A

* NATURAL ENVIRONMENT DESIGN CRITERIA FOR THE SPACE STATION PROGRAM DEFINITION AND PRELIMINARY DESIGN (FIRST REVISION)

6.0 METEOROIDS

The SSPE's will be designed to prevent loss of functional capability for all items critical to maintaining crew safety and minimum operational support. The SSPE's will otherwise be designed for at least a 0.95 probability of no penetration during the 10-year on-orbit design lifetime. The meteoroid flux model given in Figure 2-14, page 2-22, of NASA TM 82478 will be used (see section 2.6 of NASA TM 82478). It is further defined in NASA SP-8013, "Meteoroid Environment Model."

The logarithmic cumulative flux distribution model for the sporadic meteoroid population is given by the expressions:

$$a) \text{Log}_{10}N = -14.41 - 1.22 \text{Log}_{10}m; \text{ for } 10^{-6} < m \leq 10$$

$$b) \text{Log}_{10}N = -14.34 - 1.58 \text{Log}_{10}m = 0.063 (\text{Log}_{10}m)^2; \text{ for } 10^{-12} < m \leq 10^{-6}$$

where N is the cumulative flux, $m^{-2} s^{-1}$ (2π st) and m is mass, g. The sporadic flux is omnidirectional and the SSPE in orbit will be partially shielded by the Earth. The extent of the shielding is a function of altitude, and the shielded flux is equal to $(\frac{1+\cos\theta}{2})N$ where:

$$\sin\theta = \frac{R}{R+H}$$

R = Radius of the Earth

and H = altitude of SSPE above Earth's surface.

The average hourly rate of meteoroids increases at times during a calendar year due to meteoroid streams as previously noted. Their periods of activity and peak fluxes are given in Table 2-3, page 2-20, of NASA TM-82478, where F_{max} is the ratio of the stream to the sporadic meteoroid cumulative flux levels. Note that there is little or no enhancement of the sporadic population for masses less than 10^{-6} gm during stream activity.

Meteoroids are assumed to be spherical in shape and to have a bulk mass density of 0.5 gm/cc. However, this does not apply to micrometeoroids (<50 μ diameter) and it is generally assumed that a density of 2 gm/cc is more appropriate. The average atmospheric entry velocity of sporadic meteoroids is 20 km/sec, which is the value generally used to assess impact damage to spacecraft in Earth orbit. Stream meteoroids generally enter much faster as is seen in Table 2-3, page 2-20, NASA TM-82478.

Space debris has become a significant factor of concern in recent years. Since it is a man-made environment and not a natural environment parameter, it is covered elsewhere in the SSPE requirements. The flux of space debris may exceed that of

meteoroids. Therefore, NASA JSC Design Standard 20001 "Orbital Debris Environment for Space Station" should be consulted to insure that an overall SSPE design for both space debris and micrometeoroids damage protection results which will permit accomplishment of the SSPE operational requirements.

6.1 Manned Volumes and Pressure Loss

The SSP manned volume will be protected from meteoroid impact damage which would result in pressure loss that is critical to the crew's safety.

6.2 Pressure Storage Tanks

The SSPE's pressurized storage tanks will be designed to ensure no toxic gas on liquid leak from meteoroid impact damage.

6.3 Functional Capability

The probability of no penetration shall be assessed on each SSPE in terms of the criticality of loss for its functional capability.

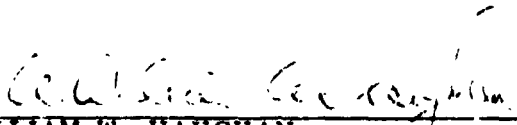
*NASA TM 86460.

APPROVAL

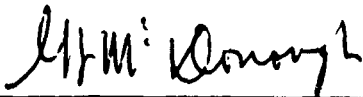
A REVIEW OF MICROMETEOROID FLUX MEASUREMENTS
AND MODELS FOR LOW ORBITAL ALTITUDES
OF THE SPACE STATION

By Michael Susko

The information in this report has been reviewed for technical content. Review of any information concerning Department of Defense or nuclear energy activities or programs has been made by the MSFC Security Classification Officer. This report, in its entirety, has been determined to be unclassified.



WILLIAM W. VAUGHAN
Chief, Atmospheric Sciences Division



G. F. McDONOUGH
Director, Systems Dynamics Laboratory